High translational energy release in H_2 (D_2) associative desorption from H (D) chemisorbed on C(0001)

S. Baouche,[a] G. Gamborg, V. V. Petrunin, A. C. Luntz, and A. Baurichter
Physics Department, University of Southern Denmark, DK-5230 Odense, Denmark

L. Hornekær
Department of Physics and Astronomy, University of Aarhus, DK-8000 Århus, Denmark

(Received 6 March 2006; accepted 13 June 2006; published online 24 August 2006)

Highly energetic translational energy distributions are reported for hydrogen and deuterium molecules desorbing associatively from the atomic chemisorption states on highly oriented pyrolytic graphite (HOPG). Laser assisted associative desorption is used to measure the time of flight of molecules desorbing from a hydrogen (deuterium) saturated HOPG surface produced by atomic exposure from a thermal atom source at around 2100 K. The translational energy distributions normal to the surface are very broad, from ~0.5 to ~3 eV, with a peak at ~1.3 eV. The highest translational energy measured is close to the theoretically predicted barrier height. The angular distribution of the desorbing molecules is sharply peaked along the surface normal and is consistent with thermal broadening contributing to energy release parallel to the surface. All results are in qualitative agreement with recent density functional theory calculations suggesting a lowest energy *para*-type dimer recombination path. © *2006 American Institute of Physics*.
[DOI: 10.1063/1.2220565]

I. INTRODUCTION

Understanding the basic mechanisms of hydrogen interacting with the surface of graphite is the key to solving a number of scientific and technological problems in fields as diverse as astrophysics, fusion reactor design, and in hydrogen storage. In astrophysics, it is well accepted that the most abundant molecule in the universe, H_2, is produced by H atom recombination on the surfaces of interstellar dust grains.[1] Although the detailed chemical nature of the grains is still somewhat uncertain, observational studies suggest grain particles made of silicates and carbon in various porous and nonporous modifications [graphite, polycyclic aromatic hydrocarbons (PAHs), amorphous carbon, and even diamond].[2] The dense molecular clouds of the interstellar medium, where stars are formed, are cold ($T \sim 10$ K), so that molecular hydrogen can only be formed by the recombination of physisorbed H on the ice mantles of grains. However, in more diffuse regions, e.g., photon dominated regions and hot cores or corinos of young stellar objects, the grains are too hot to be covered by ice and too hot to stably bind the weakly physisorbed H atoms. In these regions, chemisorbed H atoms bound to bare carbonaceous grains are viable candidates for the H_2 produced. The design of lightweight, high capacity hydrogen storage materials is one of the most challenging tasks for developing small to medium sized passenger vehicles that are powered by hydrogen fuel cells.[3,4] The low weight of carbon and the high internal surface area of its many nanostructured modifications make carbon based materials attractive candidates for hydrogen storage.

Especially in astrochemistry and hydrogen storage related research, H atom and H_2 molecule adsorption on graphite and related nanostructured materials, e.g., single- and multiwall nanotubes, were previously studied predominantly in the weakly bound physisorption state.[5,6] In contrast, this paper focuses on associative desorption from the more strongly bound chemisorption state of hydrogen atoms at the surface of highly oriented pyrolytic graphite (HOPG). The HOPG surface serves as a model surface for carbon based nanomaterials in order to assess their capability to store hydrogen at room temperature. A weak metastably chemisorbed state of H on C(0001) was predicted by electron structure calculations.[7–9] In this state, the H is bonded atop to a single C atom which puckers out of the plane by ca. 0.35 Å and exhibits essentially sp^3-type bonding rather than the usual sp^2 bonding of graphite.[8,10,11] An overview of the adiabatic energetics of the minimum energy path for adsorption and desorption of H and H_2 from this chemisorbed state on C(0001) is presented in Fig. 1. This path is synthesized from what we believe are the most accurate density functional theory calculations (DFT) available for the system.[12,13] All adsorbed states and barriers are for fully relaxed atomic geometries, including puckering coordinates of the C lattice. In order to adsorb hydrogen molecules dissociatively onto the basal planes of graphite, two nearby carbon atoms need to move simultaneously out of the basal plane. This is energetically unfavorable and exhibits a minimum barrier of 3.4 eV.[13–15] It is therefore virtually impossible to produce the H chemisorbed state via dissociation of H_2 on C(0001). On the other hand, adsorption of gas phase H atoms into the chemisorbed state exhibits much smaller barriers, around 0.2 eV.[7,8] The binding energy of the H at low hydrogen coverage is ~0.7 eV.[8,12] The barrier for adding a second H atom nearby to a chemisorbed H is unknown (question mark in

[a]Electronic mail: baouche@fysik.sdu.dk

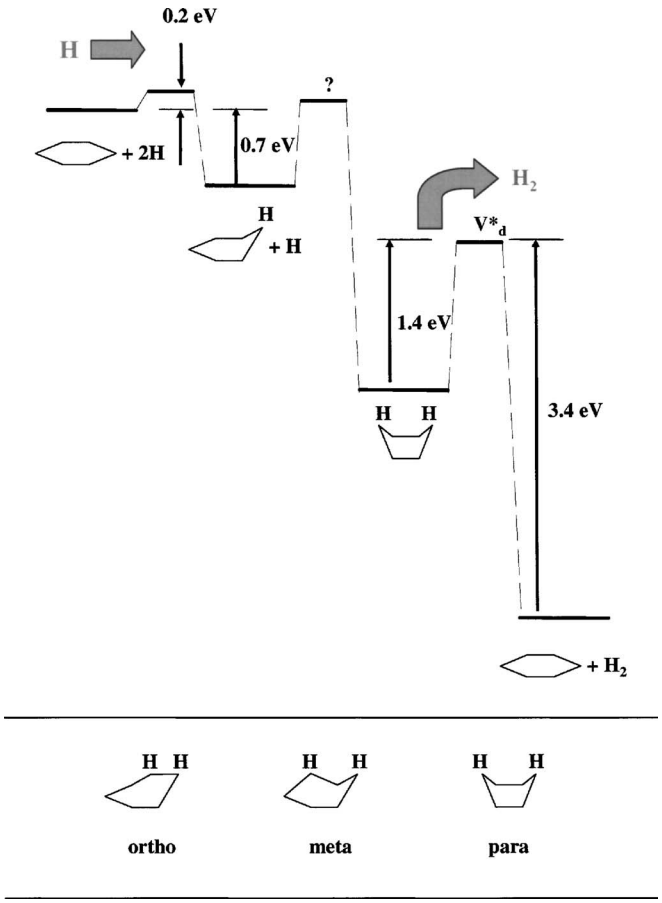

FIG. 1. Schematic one-dimensional potential energy diagram for hydrogen atom adsorption and molecular desorption at the basal planes of HOPG graphite. The energies are partly from DFT calculations and partly from experimental data. The question mark indicates the lack of theoretical and experimental data on the barrier height for atomic sticking into the *para* configuration in the presence of another hydrogen atom chemically bound to the surface (see text). The nomenclature used for the different hydrogen associative desorption pathways are depicted at the bottom of the figure.

Fig. 1). The DFT calculations also show that there are strong attractive lateral interactions between adsorbed H atoms, so that the thermodynamic minimum energy configuration for chemisorbed H atoms at higher coverage is as dimers or even larger clusters.[13,15,16] There are three different dimer configurations, with the two H atoms located *ortho, meta*, or *para* on a given hexagonal ring that form the basal plane of graphite (see bottom of Fig. 1).[13,15,17] The *para* and *ortho* dimers are the most stable, and the *para* dimer has the lowest barrier to associative desorption.[13] This associative desorption path is sketched in Fig. 1. All dimer states are only metastable with respect to associative desorption of H_2 stabilized by a barrier to desorption, which in the case of the *para* dimer has a height of 1.4 eV.

Due to the adsorption barriers involved, hydrogen chemisorption on the defect-free basal plane of graphite was not proved to exist experimentally until recently. Zecho *et al.*[12] demonstrated that hydrogen atoms from a 2000 K hot W surface dissociation source have sufficient kinetic energy to surmount the atomic adsorption barrier and bind chemically to the basal planes of HOPG. By combining temperature programmed desorption (TPD) experiments with electron energy loss spectroscopy (ELS), high-resolution energy loss spectroscopy (HREELS), they estimated a net sticking probability between 0.25 and 0.5 for 2000 K thermal H and D atoms and a maximum H (D) coverage Θ per C atom of $\Theta = 0.4 \pm 0.2$. The fact that no H (D) adsorption is observed at lower temperatures of the incident atoms is compatible with the theoretically predicted H (D) adsorption barrier of 0.2 eV. The main thermal desorption feature for H_2 (D_2) at $T \approx 450$ K (490 K) arises from associative desorption of the chemisorbed H (D) atoms. The thermal desorption exhibits unusual first order reaction kinetics. Very recent scanning tunneling microscopy experiments on H/C(0001) confirm the formation of agglomerates of H into clusters ranging from two and more hydrogen atoms and suggest that this is the reason for the first order desorption kinetics,[13] in a manner similar to the first order desorption kinetics of H_2 from diamond C(111)[18] and other covalently bound surfaces as Si(100).[19,20]

One issue of considerable importance in both astrochemistry and in hydrogen storage is the disposal of the H_2 recombination energy as the molecule is formed, i.e., the partitioning of 3.4 eV into H_2 translation, vibration, and rotation and into the C(0001) lattice. In astrochemistry, this partitioning impacts models of photodissociation regions. Observations show that a substantial fraction of molecular hydrogen in these regions is in highly excited rovibrational states. Some of this excitation is believed to be due to the formation of hydrogen molecules in highly excited states.[21–23] In hydrogen storage, the partitioning could influence how the additional energy storage of the metastable chemisorbed species is utilized. In this paper we report measurements of the translational energy distribution of hydrogen and deuterium molecules associatively desorbing from the surface of graphite from the chemisorbed state. These measurements are based on the technique of laser assisted associative desorption (LAAD). In this technique, molecular recombination and desorption is thermally induced by a temperature jump (T-jump) generated by surface absorption of pulsed laser radiation in the near infrared. The translational energy distribution is obtained from the time of flight distribution (TOF) of the H_2 (D_2) from the surface to a mass spectrometer. This technique has been successfully utilized previously in the study of associative desorption of catalytically important systems on metal surfaces.[24–26] We find that on average about 1/3 of the available energy of 3.4 eV is partitioned into translational energy normal to the surface. The energy distribution is broad, peaking at 1.3 eV, and tails out to ~3 eV. Angularly resolved detection shows that essentially none of the 3.4 eV barrier energy is partitioned into translational energy parallel to the surface. The results imply that a considerable amount of the desorption energy (~2/3) is partitioned into H_2 (D_2) vibration and/or surface degrees of freedom.

II. EXPERIMENT

All experiments are carried out in an ultrahigh vacuum (UHV) chamber equipped with standard surface science instrumentation. A detailed description of the apparatus can be found in Refs. 25 and 27. A 1 mm thick, 9 mm diameter

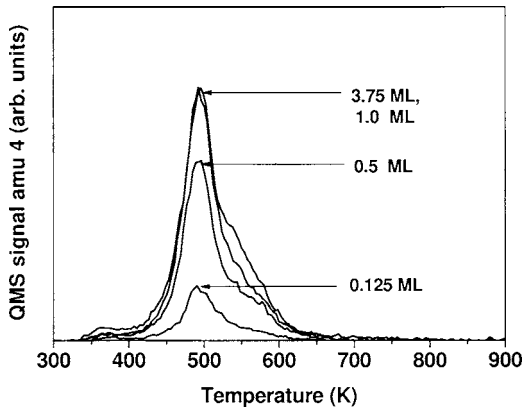

FIG. 2. TPD data of D_2 desorption from C(0001) after D atom dosing at room temperature with 2×10^{13} at./cm^2 s.

HOPG disk is attached to a tantalum plate of 2 mm thickness by a ceramic glue.[28] The C/Ta is mounted to a water cooled sample manipulator. The C(0001) is heated from the back side by electron beam impact onto the Ta backing. A type-C thermocouple is glued to the rim of the HOPG for temperature measurements and calibrated by a focusing IR probe. Prior to introduction into the UHV system, the HOPG is cleaved in air with adhesive tape. The vacuum system is subsequently baked to achieve UHV. Before each experiment, the HOPG surface is cleaned by annealing at 1350 K for 30 s. For hydrogenation, the sample is exposed to hydrogen or deuterium atoms from a hot tungsten capillary thermal cracker source of the Jülich type.[29] A typical flux density of $10^{13}-10^{14}$ at./s cm^2 is achieved at the position of the sample surface, ca. 18 cm from the exit of the W capillary. A capillary temperature of 2100 K is chosen in order to provide a dissociation efficiency of >95% and sufficient energy to surmount the adsorption barrier of ~0.2 eV. TPD experiments are performed after translating the HOPG surface to within 1.5 mm of the opening of a Feulner cap[30] entrance to a differentially pumped quadrupole mass spectrometer. Typical heating rates for the TPD are 1–3 K/s, and TPD was routinely used to monitor the surface quality of the HOPG sample (Fig. 2).

In LAAD, a pulsed infrared laser induced T-jump causes associative desorption from the surface. Because the laser is pulsed, surface heating also occurs only for a short time. The translational energy distribution of desorbing molecules is obtained by measuring the TOF distribution of the desorbing species with a differential pumped mass spectrometer, the ionizer of which is located at a distance of ~10 cm from the surface. An Alexandrite laser at 760 nm wavelength and temporal pulse width of 150 ns or a Nd:YAG (yttrium aluminum garnet) laser at 1064 nm with a temporal width of 17 ns have been used with essentially the same LAAD results. Both lasers have a 10 s^{-1} repetition rate. Imaging of the Alexandrite laser onto the surface produced illuminated spots of 1.3 mm (Nd:YAG: 1.5 mm) diameter with a nearly Gaussian spatial distribution. Since the Alexandrite laser was mostly used for the experiments in this paper, all laser pulse energy densities given refer to 150 ns pulse length and beam diameters of 1.3 mm, unless otherwise stated. The incident angle of the laser to the surface is ~45° and the illuminated spot is therefore somewhat elliptically shaped on the sample surface. Under conditions where the T-jump induces only weak desorption per laser pulse, the LAAD is well approximated by isothermal desorption at a temperature corresponding to the peak temperature of the T-jump.[25] The state integrated desorption rate can thus be described by the simple rate equation,

$$-\frac{d\Theta}{dt}=\nu\,\Theta^n\exp\left(\frac{-E_{\mathrm{des}}}{k_BT(t)}\right), \tag{1}$$

with Θ the surface coverage, ν the pre-exponential factor, and E_{des} the desorption energy. In the case of hydrogen associative desorption from HOPG, Zecho *et al.*[12] found a reaction order of $n=1$. Therefore, LAAD can be understood as conventional TPD but with an ultrafast temperature ramp of $10^{10}-10^{12}$ K/s. The Boltzmann factor dictates the strong temperature dependence of the desorption rate and the vast majority of molecules will be desorbed around the peak temperature. Conventional thermal modeling[31] of the T-jump shows that the surface temperature reaches its peak with only a small delay relative to the laser pulse (<100 ns for the Alexandrite laser) and that its duration is ~100 ns. Its magnitude depends on laser intensity. The peak temperature in the T-jump is thus readily controlled by varying the laser intensity. Repeated laser shots at a given surface spot ultimately bleach the signal due to inducing associative desorption from the T-jump. By monitoring the bleaching curve, the number of desorbed molecules per laser shot is estimated. For the two laser intensities used in the experiments reported here, 150 and 400 mJ/cm^2, desorption yields are typically of the order of 0.01 and 0.1 ML/pulse, respectively. These yields are small enough that the LAAD is well approximated as an isothermal desorption at the peak temperature of the T-jump. After bleaching at one laser spot area, the sample is moved parallel to its surface to expose another irradiation area that does not overlap with the previous one. A total number of 7–18 spots are visited in this way on the sample and LAAD results are averaged for all laser shots and different spots.

The translational energy distributions of H_2 (D_2) desorbing along the surface normal from a H (D) covered HOPG measured with LAAD do not exhibit any detectable temperature dependence on the peak temperature in the T-jump, as will be shown in a later paragraph (see Fig. 3). Only the width of the angular distribution is affected by weak broadening upon increasing the temperature (Fig. 4). While this weak temperature dependence will be discussed in the later section of this paper, the maximum surface temperature in the T jump of the LAAD is estimated here in three different ways. First, a three-dimensional solution of the heat equation describing the surface T-jump induced by optical absorption of the laser pulse is performed. This gives peak T-jumps of 900 K at 150 mJ/cm^2 laser pulse energy density and 1900 K at 400 mJ/cm^2. An uncertainty of ±15% of the peak temperature lies in the spread of literature values of graphite thermal conductivity normal to the planes, presumably due to sample to sample variability.[32] Secondly, the peak temperature can be estimated from the desorption yield per laser pulse by comparing the desorption rate of LAAD with

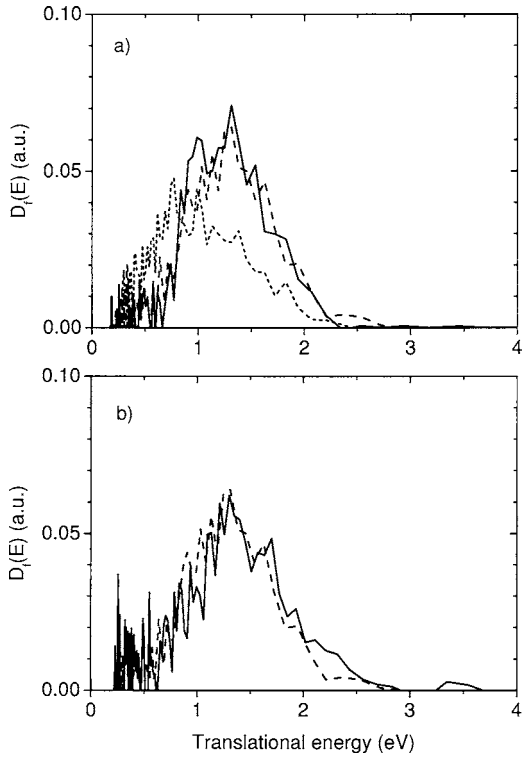

FIG. 3. Translational energy distributions $D_f(E)$ from LAAD of D_2 and H_2, desorbing from C(0001). The dependence of the $D_f(E)$ of D_2 on laser pulse energy density is shown in (a). The solid line corresponds to 150 mJ/cm^2, the dashed line to 400 mJ/cm^2, and the dotted line shows desorption from defects at 400 mJ/cm^2 after annealing the surface for 30 s at 650 K. The isotope dependence of $D_f(E)$ is shown in (b), for H_2 (solid line), and D_2 (dashed line). Both data sets are recorded at 400 mJ/cm^2.

TPD. Assuming an exponential bleaching of the H (D) coverage in the beam spot, about $\Delta\Theta \approx 0.01\Theta_s$ of the saturation coverage Θ_s is desorbed in LAAD on the first laser shot at 150 mJ/cm^2. The typical temperatures T_{LAAD} at which this desorption occurs on the time scale of the LAAD experiment can be estimated according to Eq. (1), provided laser assisted desorption probes the same desorption channel as TPD, i.e., across the minimum energy barrier. In TPD, D_2 desorption of $\Delta\Theta = 0.01\Theta_s$ occurs on a time scale of $\Delta t \approx 1$ s at around 500 K, whereas the same coverage change occurs on a time scale of $\Delta t \approx 100$ ns in LAAD. The temperature T_{LAAD} required for desorbing the same amount of coverage $\Delta\Theta$ in a LAAD experiment as in the TPD can be estimated by comparing the rate equations (1):

$$\frac{-\Delta\Theta/\Delta t_{\mathrm{LAAD}}}{-\Delta\Theta/\Delta t_{\mathrm{TPD}}} = \frac{\Delta t_{\mathrm{TPD}}}{\Delta t_{\mathrm{LAAD}}} = \frac{\exp(-E_{\mathrm{des}}/k_B T_{\mathrm{LAAD}})}{\exp(-E_{\mathrm{des}}/k_B T_{\mathrm{TPD}})} \tag{2}$$

or

$$T_{\mathrm{TPD}}/T_{\mathrm{LAAD}} = 1 - \frac{k_B T_{\mathrm{TPD}}}{E_{\mathrm{des}}} \ln \frac{\Delta t_{\mathrm{TPD}}}{\Delta t_{\mathrm{LAAD}}}. \tag{3}$$

For $E_{\mathrm{des}} = 1.4$ eV one gets $T_{\mathrm{LAAD}} \approx 2T_{\mathrm{TPD}}$, or $T_{\mathrm{LAAD}} \approx 1000$ K, which is in reasonable agreement with the result of the first method.

The third method is based on the observation that carbon hydrides desorbing from edge related defects desorb with a Maxwell-Boltzmann translational energy distribution which depends on the laser intensity. Although the mechanism for formation of the carbon hydrides is unknown, we assume that they desorb in equilibrium with the surface. Because the carbon hydrides desorb only at higher temperatures than H_2 from the basal plane[33] this was measured for the higher laser intensity (400 mJ/cm^2) and gave $T = 2400$ K for C_2D_4 desorption. Finally, we note that the thermal broadening caused by the T-jump is negligible in the energy partitioning compared to the ~3.4 eV released in the associative desorption.

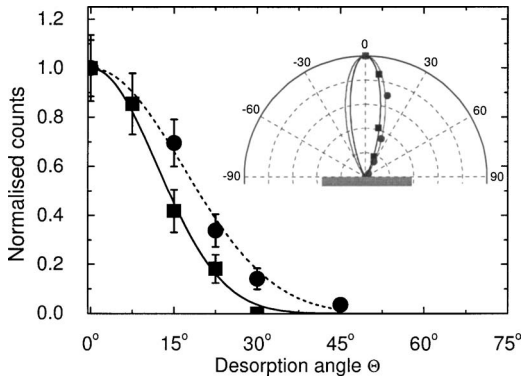

FIG. 4. Angular distributions of D_2 LAAD from C(0001). The square symbols label desorption at a laser pulse energy of 150 mJ/cm^2, and the circles represent desorption at 400 mJ/cm^2. The lines are $\cos^n(\Theta)$– fits to the data, where Θ denotes the angle from the surface normal, and $n = 23$ (solid line), and $n = 13$ (dashed line). The inset shows a polar plot of the same data with the HOPG surface indicated as a gray bar.

Following the argumentation of Diekhöner *et al.*[25] and Luntz[26] the translational energy of molecules normal to the surface (E) in thermal associative desorption from the surface is given as

$$E \approx V_d^* + \langle E_{\mathrm{th}}^* \rangle + \tfrac{1}{2} k_B T_s - E_{\parallel} - E_v - E_j - E_s, \tag{4}$$

with V_d^* the adiabatic zero point corrected dissociative adsorption barrier (~3.4 eV, see Fig. 1), $\langle E_{\mathrm{th}}^* \rangle$ the thermal energy in the transition state in vibrational modes perpendicular to the reaction coordinate, $\frac{1}{2} k_B T_s$ the thermal energy in the reaction coordinate caused by the final thermal fluctuation causing associative desorption, $E_{\parallel}$ the translational energy parallel to the surface, E_v and E_j the vibrational and rotational energies of the nascent molecule, and E_S the energy loss to the surface upon desorption. The translational energy distribution thus reflects the internal state distribution of the desorbing molecules and the energy loss to the lattice as well as the energy barrier to dissociation.

TOF are recorded by detecting the molecules desorbing by means of a second differentially pumped quadrupole mass spectrometer mounted on a rotating stage. For all experiments reported here, except the angular distribution measurements, the TOF is measured when the detector is placed normal to the surface. The ionization region of this mass spectrometer is located at a distance of 97 mm from the sample surface. Both the surface-ionizer distance l and the insertion delays of the detection system have been calibrated by recording TOF for LAAD at different l and overlaying the velocity distributions. For ultimate theoretical comparisons, the flux weighted translational energy distribution normal to the surface $D_f(E)$ is important. The LAAD data are collected

as density weighted time-of-flight distributions $n(t)$ and can be converted to $D_f(E)$ by $D_f(E)=\text{const}\, t^2 n(t)$ with $E=\frac{1}{2}ml^2(t_0-t)^{-2}$, with m the mass of the molecule, l the sample-ionizer distance, t the flight time, and t_0 the sum of all insertion delays. Because of a variety of detection variables, only the E dependence of $D_f(E)$ is meaningful. The absolute magnitude of $D_f(E)$ is uncertain.

The detector is simply rotated to measure the angular distributions of molecules desorbing from the surface. In this way, the dimensions of the beam spot and therefore the T-jump remain the same as the angular distribution is measured. The angular resolution, defined by the aperture of the differentially pumped detector, is $\sim 1°$. For each measured angle, the TOF was integrated and normalized to the total number of laser pulses used to give the total desorption yield $Y(\theta)$ at a given angle θ relative to the surface normal.

III. RESULTS AND DISCUSSION

TPD spectra after varying doses of atomic D are shown in Fig. 2. The same features and saturation of the TPD intensity with dose are observed as reported earlier by Zecho *et al.*[12] When edge-type defects are present, H_2 (D_2) desorption also occurs over a broad range from ca. 650 to 1000 K and carbon hydrides are simultaneously desorbed in the same temperature region.[33] We have observed for a given cleaving of the HOPG, or in subsequent treatments, that there is no guarantee that a low density of step edges is maintained. We therefore use TPD spectroscopy routinely to survey the surface quality of our sample.

There are at least two dominant peaks in the TPD spectra at 450 K (490 K) and 560 K (580 K) for H_2 (D_2) desorption. These were earlier shown to result from H (D) adsorption on the basal plane and are not defect related.[33] A simple Redhead analysis of the dominant peak in the TPD of H_2 associative desorption from C(0001) gives a barrier of ~ 1.4 eV, assuming a normal pre-exponential factor for desorption of $\sim 10^{13}\ \text{s}^{-1}$. This is in excellent agreement with most recent DFT calculations of the barrier using a much larger unit cell as earlier calculations[13] (see Fig. 1). Note that an earlier estimate of the barrier to desorption based on a leading edge analysis of the TPD spectra gave a substantially lower value.[12]

Recent STM experiments coupled with DFT calculations suggest that at low Θ_H (Θ_D), the two peaks in the TPD correspond to associative desorption from two types of dimers.[13] The main peak at 450 K (490 K) is due to desorption of the dominant *para*-type dimer, while the peak at 560 K (590 K) results from the *ortho* dimer which through diffusion converts to the *para* dimer before associatively desorbing. As Θ_H (Θ_D) increases, large clusters are apparently formed. Since no new peaks are formed in the TPD, and it is unlikely that associative desorption barriers are identical in large clusters as for the dimers, we suggest that desorption in those clusters occurs through the same reaction path.

D_2 translational energy distributions $D_f(E)$ normal to the surface obtained by LAAD after the HOPG surface has been saturated with chemisorbed D are shown in Fig. 3 for two different laser pulse energy densities of 150 and 400 mJ/cm^2, corresponding to estimated peak T-jumps of 900 and 1900 K, respectively. The lower pulse energy corresponds to the detection threshold for associative desorption from the basal planes. The E dependence of the distributions is identical within experimental accuracy. The distributions are broad, extending from ca. 0.5 eV to almost 3 eV and peak at ~ 1.3 eV. Several LAAD experiments with more defected samples than those evidenced in Fig. 2 and Fig. 3were also measured and gave identical LAAD at laser intensities of 150 mJ/cm^2. In order to make sure that the LAAD corresponds to associative desorption from the basal planes, TPD spectra were recorded after fully depleting the laser irradiated surface areas with a 150 mJ/cm^2 laser pulse energy density (~ 250 laser pulses/spot). The basal plane TPD peak at ~ 500 K decreases in intensity by the ratio of the total beam spot areas to the total sample area. No decrease of the defect related TPD peaks at $T>650$ K is observed. However, annealing a deuterium covered HOPG surface with significant defects for 5 s to 670 K and using a higher laser intensity of 400 mJ/cm^2 gives a substantially different $D_f(E)$ shifted to significantly lower E, presumably related to preferential desorption from edge related defect sites. We also note that in the bleaching studies, no desorption signal is observed after waiting several minutes and then revisiting the totally bleached beam spots. This indicates that there is no macroscopic diffusion of chemisorbed D at 300 K.

Neglecting tunneling, the average total energy release in associative desorption from the chemisorbed state along the minimum energy path [see Fig. 1 and Eq. (4)] is $V_d^*+\langle E_{\text{th}}^*\rangle$, with $V_d^*=3.4$ eV and $\langle E_{\text{th}}^*\rangle$ the thermal energy in the transition state. Since $V_d^* \gg \langle E_{\text{th}}^*\rangle$, and $D_f(E)$ is found to be experimentally almost independent of the peak temperature in the T-jump (laser pulse energy density), we neglect the thermal energy term. Thus, $E+E_\parallel+E_\nu+E_J+E_S \approx 3.4$ eV, where $E_\parallel$ is the translational energy parallel to the surface, E_ν is the vibrational energy in the desorbed molecule, E_j is its rotational energy, and E_s is the energy deposited into the surface as either phonons or electronic excitation (electron-hole pairs) as a result of release of V_d^* in associative desorption. Because of the broad distribution in E, there must be a correspondingly broad distribution, either in other molecular degrees of freedom or in surface excitations as well. We have measured on average a strong energy release of $\langle E\rangle \approx 1.3$ eV into translation normal to the surface, but this only accounts for roughly 40% of all energy release.

In order to probe the energy partitioning into $E_\parallel$, the angular distributions for D_2 associative desorption were measured under the same initial conditions as used in Fig. 3 (Fig. 4). The desorption is clearly sharply peaked normal to the surface. The width of the angular distribution depends on the laser energy density and hence peak surface temperature in the T jump. Fitting the desorption angular distributions to $\cos^n(\theta)$ distributions yield $n=23$ for a pulse energy density of 150 mJ/cm^2 ($T_s \approx 900$ K) and $n=13$ for 400 mJ/cm^2 ($T_s \approx 1900$ K), respectively. The width of the angular distribution and its temperature dependence can be explained qualitatively by assuming that the D_2 only picks up transverse momentum during the formation process due to thermal motion in the transition state, i.e., from $\langle E_{\text{th}}^*\rangle$. The mag-

nitude of this effect is estimated by expressing the half width of the angular distribution by $\theta_w = \arctan(\sqrt{k_B T_s / 2\langle E \rangle})$ with $\langle E \rangle$ the average translational energy of the molecules desorbing into the normal direction and $\frac{1}{2}k_B T_s$ the average energy of the motion parallel to the surface. For $T_s = 900$ K a width of 10° is obtained from this model and 14° for 1900 K. Both angles are in acceptable agreement with the experiment (14° and 20°, respectively). Similarly, the contribution of $\langle E^*_{\text{th}} \rangle$ to E leads to an insignificant broadening of the translational energy distribution relative to that produced by release of V^*_d.

None or at most a negligible amount of V^*_d is partitioned into $E_\parallel$. This conclusion is fully consistent with DFT calculations of the minimum energy path for desorption from the *para* dimer state.[15,13] The path is fully symmetric with respect to the surface normal, so that the potential energy released in directions parallel to the surface is anticipated to be negligible. In addition, from the symmetry of the path it is anticipated that no torque is exerted on the desorbing H_2 (D_2) so that we also expect that there is minimal rotational excitation E_j occurring by release of the energy stored in V^*_d. There will, however, be some rotational excitation from $\langle E^*_{\text{th}} \rangle$ which will be of the order of $k_B T_s$ and thus is expected to be much smaller than the total vibrational excitation. Because $\langle E \rangle \ll 3.4$ eV, $\langle E_v + E_S \rangle$ must then account for ~60% of the energy release. The results reported here cannot separate these two contributions. From the DFT calculations, both are viable candidates. At the transition state, the H–H bond is significantly stretched, $d_{\text{HH}} = 1.3$ Å relative to the free molecule $d_{\text{HH}} = 0.745$ Å.[15] As the molecule desorbs energy should be released into molecular vibration E_v. In a similar manner, the two C atoms forming the H atom bonds are significantly puckered out of the C(0001) plane by ~0.45 Å at the transition state.[34] Release of this puckering energy could give significant lattice excitation and contribute to E_S. Finally, because H adsorption breaks the delocalized two-dimensional π bonding of the graphene sheets, associative desorption of H_2 could produce strong nonadiabatic electronic rearrangements and hence cause dissipation via creation of electron-hole pairs.[35] This could also contribute to E_S.

We have measured the isotope effect in $D_f(E)$, in part to compare to the large isotope effect observed in TPD and in part to probe whether this provides any evidence as to whether E_v or E_S is a dominant term in the energy partitioning. Figure 3(b) shows $D_f(E)$ for H_2 and D_2 at a laser energy density of 400 mJ/cm^2. The results are normalized to each other because absolute desorption intensities have many experimental variables. There is no measurable difference in the E dependence of the two isotopes. This suggests that V^*_d is essentially the same for the two isotopes. The isotope effect in TPD could arise in part from differences in preexponential factors in the kinetic equations for desorption. At this stage, we can only speculate about the relationship of the lack of an isotope effect in $D_f(E)$ to energy partitioning in associative desorption. Certainly one anticipates little isotope effect if E_v is the remaining dominant energy loss channel. On the other hand, it is possible but by no means certain that isotope effects could result from both lattice and electron-hole pair contributions to E_S.

It is possible to more definitively probe energy partitioning in associative desorption by combining LAAD with state resolved detection techniques, e.g., resonance enhanced multiphoton ionization (REMPI).[36] Experiments are currently underway in our laboratory to measure the full partitioning of H_2 desorption from C(0001) and will be reported later. However, preliminary state resolved LAAD experiments show that some low vibrational states are produced in associative desorption with significant loss to E_S.

IV. SUMMARY AND CONCLUSIONS

Using the technique of LAAD, we have measured the translational energy distributions $D_f(E)$ of H_2 and D_2 associatively desorbing from chemisorbed states of H (D) on HOPG normal to the surface at saturation coverage. The distributions are quite broad, from 0.5–3 eV, and peak at $\langle E \rangle \approx 1.3$ eV. By combining the measurement of the angular distributions for associative desorption with $\langle E \rangle$, we show that only thermal energy at the transition state emerges as energy parallel to the surface. None of the potential barrier is partitioned into energy parallel to the surface. This confirms that the reaction path for associative desorption from the transition state to the desorbed molecule remains normal to the surface throughout, in full agreement with DFT calculations of the minimum energy path.[15,13] Since the total energy released in associative desorption is ~3.4 eV according to DFT calculations,[13] on average considerable energy must also be partitioned into H_2 (D_2) vibration and/or the C(0001) surface. We believe that this energy partitioning has implications for both astrochemistry and in how the extra energy due to the metastability of H adsorbed on C(0001) can be utilized in carbon based hydrogen storage.

ACKNOWLEDGMENTS

The authors wish to thank Thomas Zecho for discussions and his help during the startup of the experiments. This work was supported by The Danish Natural Science Research Council (Grant No. 21030445). One of the authors (L.H.) acknowledges support from The Carlsberg Foundation.

[1] D. Hollenbach and E. E. Salpeter, Astrophys. J. **163**, 155 (1971).
[2] E. Kruegel, *The Physics of Interstellar Dust* (Institute of Physics, Bristol, UK, 2003), and references therein.
[3] L. Schlapbach and A. Züttel, Nature (London) **414**, 353 (2001).
[4] US Department of Energy, Office of Basic Energy Sciences, *Basic Research Needs for the Hydrogen Economy* (US DOE, Washington, DC, 2004), available at http://www.sc.doe.gov/bes/hydrogen.pdf; Basic Energy Sciences Advisory Committee, *Basic Research Needs to Assure a Secure Energy Future* (US DOE, Washington, DC, 2003), available at http://www.sc.doe.gov/bes/reports/files/SEF_rpt.pdf; Committee on Alternatives and Strategies for Future Hydrogen Production and Use, *The Hydrogen Economy: Opportunities, Costs, Barriers, and R&D Needs*, (National Academy Press, Washington, DC, 2004), available at http://www.nap.edu/catalog/10922.html
[5] M. Hirscher and M. Becher, J. Nanosci. Nanotechnol. **3**, 3 (2003).
[6] C. Liu and H. M. Cheng, J. Phys. D **38**, R231 (2005).
[7] L. Jeloaica and V. Sidis, Chem. Phys. Lett. **300**, 157 (1999).
[8] X. W. Sha and B. Jackson, Surf. Sci. **496**, 318 (2002).
[9] Y. Ferro, F. Marinelli, and A. Allouche, J. Chem. Phys. **116**, 8124 (2002).
[10] Y. Miura, H. Kasai, W. A. Dino, H. Nakanishi, and T. Sugimoto, J. Phys. Soc. Jpn. **72**, 995 (2003).
[11] X. W. Sha, B. Jackson, D. Lemoine, and B. Lepetit, J. Chem. Phys. **122**, 014709 (2005).

[12] T. Zecho, A. Guttler, X. W. Sha, B. Jackson, and J. Kuppers, J. Chem. Phys. **117**, 8486 (2002).
[13] L. Hornekaer, Z. Sljivancanin, W. Xu, R. Otero, E. Rauls, I. Stensgaard, E. Laegsgaard, B. Hammer, and F. Besenbacher, Phys. Rev. Lett. **96**, 156104 (2006).
[14] Y. Ferro, F. Marinelli, and A. Allouche, Chem. Phys. Lett. **368**, 609 (2003).
[15] Y. Miura, H. Kasai, W. Dino, H. Nakanishi, and T. Sugimoto, J. Appl. Phys. **93**, 3395 (2003).
[16] A. Allouche, Y. Ferro, T. Angot, C. Thomas, and J. M. Layet, J. Chem. Phys. **123**, 124701 (2005).
[17] The notation in this paper differs from the notation used by Hormekær *et al.* and Miura *et al.* Hornekær *et al.* name the associative desorption path via the *para* configuration *B* state, *ortho* is called *A* and *meta I*, whereas in Miura *et al. Para* is called *T-H-T* state, *ortho T-B-T*, and *meta T-C-T*.
[18] C. Su, K. J. Song, Y. L. Wang, H. L. Lu, T. J. Chuang, and J. C. Lin, J. Chem. Phys. **107**, 7543 (1997).
[19] J. J. Boland, Phys. Rev. Lett. **67**, 1539 (1991).
[20] M. Durr, A. Biedermann, Z. Hu, U. Hofer, and T. F. Heinz, Science **296**, 1838 (2002).
[21] D. Hollenbach and C. F. McKee, Astrophys. J. **342**, 306 (1989).
[22] M. G. Burton, M. Bulmer, A. Moorhouse, T. R. Geballe, and P. Brand, Mon. Not. R. Astron. Soc. **257**, P1 (1992).
[23] D. R. Flower and G. P. d. Forets, Mon. Not. R. Astron. Soc. **247**, 500 (1990).
[24] L. Diekhoner, H. Mortensen, A. Baurichter, A. C. Luntz, and B. Hammer, Phys. Rev. Lett. **84**, 4906 (2000).
[25] L. Diekhoner, H. Mortensen, A. Baurichter, and A. C. Luntz, J. Chem. Phys. **115**, 3356 (2001).
[26] A. C. Luntz, J. Chem. Phys. **113**, 6901 (2000).
[27] A. C. Luntz, M. D. Williams, and D. S. Bethune, J. Chem. Phys. **89**, 4381 (1988).
[28] Aremco Products, Inc., Valley Cottage, NY.
[29] K. G. Tschersich and V. von Bonin, J. Appl. Phys. **84**, 4065 (1998).
[30] P. Feulner and D. Menzel, J. Vac. Sci. Technol. **17**, 662 (1980).
[31] J. F. Ready, *Effects of High-Power Laser Radiation* (Academic, New York, 1971).
[32] C. Uher, *Condensed Matter (Historical Archive)*, Landolt-Börnstein, Group III, (Springer, New York, 1991).
[33] T. Zecho, A. Guttler, and J. Kuppers, Carbon **42**, 609 (2004).
[34] E. Rauls (private communication).
[35] A. C. Luntz and M. Persson, J. Chem. Phys. **123**, 074704 (2005).
[36] L. Diekhoner, L. Hornekaer, H. Mortensen, E. Jensen, A. Baurichter, V. V. Petrunin, and A. C. Luntz, J. Chem. Phys. **117**, 5018 (2002).